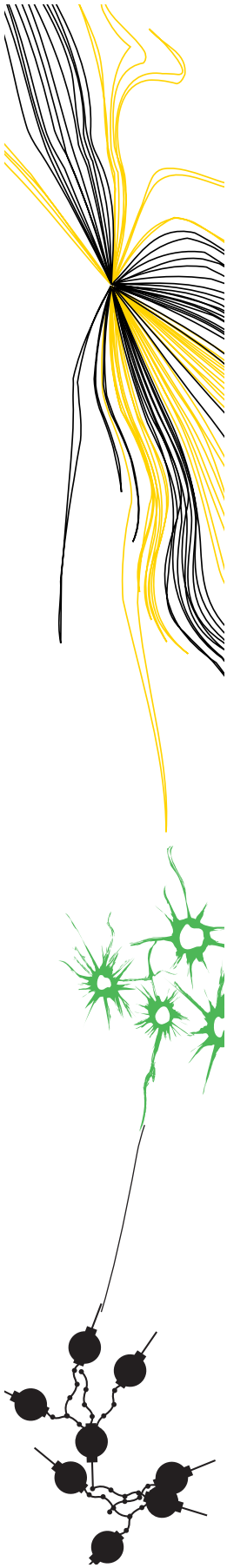

ROBOTICS AND MECHATRONICS

# CHARACTERIZATION OF ELECTRICAL PROPERTIES OF DIRECT INK WRITTEN SILVER-INK

J.P. (Jelle) Idzenga

BSC ASSIGNMENT

**Committee:**
prof. dr. ir. G.J.M. Krijnen
ir. D. Kosmas
H.R. Jonkers, MSc
dr. R. Saive

July, 2022

034RaM2022
Robotics and Mechatronics
EEMCS
University of Twente
P.O. Box 217
7500 AE Enschede
The Netherlands

UNIVERSITY OF TWENTE. | TECHMED CENTRE

UNIVERSITY OF TWENTE. | DIGITAL SOCIETY INSTITUTE

# Characterization of direct ink writing with silver-ink

Jelle Idzenga

August 22, 2022

# Contents

# 1 Paper

# Characterization of Electrical Properties of Direct Ink Written Silver Ink

Jelle Idzenga, Dimitris Kosmas, Heime Jonkers, Gijs Krijnen
Robotics And Mechatronics group, University of Twente, Enschede, The Netherlands
Email: d.kosmas@utwente.nl

***Abstract* - Direct-Ink Writing (DIW), in conjunction with Multi-Material (MM) Fused-Filament-Fabrication (FFF) was used to characterize the electrical- and piezo resistive properties of silver-ink based traces on top of thermoplastic polyurethane (TPU) substrates. Resistivity of 3D printed conducting traces is reduced by a factor of a $5 \cdot 10^5$. However, at strains above $10\,\%$ the silver ink traces showed non-linear piezoresistive behaviour. Even though silver ink was not deemed suitable for piezo-electrical sensing, the exhibited low resistivity can be used for conductive contact traces when combined with FFF printed black carbon doped polymers, as to realize 3D printed strain gauges.**

*Keywords - 3D Printed Sensors, Fused Deposition Modelling, Direct-ink writing, Silver ink, Strain gauge*

## I. Introduction

Additive manufacturing (AM) of electrically conductive materials shows potential for numerous applications in sensor development [1]. The most common 3D printing methods, FFF and SLA (Stereolithopgraphy), realize a 3D object by depositing layers of material [2]. This layer-by-layer manufacturing method enables production of complex structures and a high degree of design freedom at low cost in short time.

FFF, when employed with multi-material printing, has been demonstrated to be able to produce sensing structures [3]–[5]. However problems stemming from the layer-by-layer fabrication process occur which results in voids and defects in between layers, causing anisotropy in the resulting printed structure. In addition, the materials usable for FFF are limited to thermoplastics which, even when doped with conductive entities, have high electrical resistivity with large influence of the conductive traxels (track-elements) [4], [6]. Direct ink writing is a useful manufacturing process, especially in combination with FFF in order to print conducting inks in a flexible thermoplastic structure. In direct-ink writing, a liquid ink with specific rheological properties [7] is extruded through a nozzle. After printing, a curing process based on either a heat or an UV treatment has to be applied. These liquid inks allow for a wider range of materials, with higher conductivity than (doped) thermoplastics. In addition, as a layer is not fully solidified while the next layer is applied, a better interlayer mixing and bond can occur. As a result, the interlayer resistance will be comparable to the inlayer resistance and a lower anisotropy could be achieved [8].

In this work, silver ink is characterized for use as contact traces or for piezoresistive sensing, and the latter is determined by examining the resistive response and contact resistance upon straining.

## II. Methodology

### A. Design

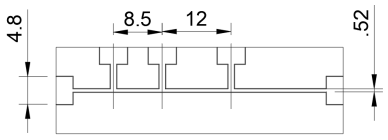


Fig. 1. Transfer length method design, dimensions in [mm]

Figure 1 shows the design for characterization of the resistivity. With the contact pads at the sides used for current injection, the 3 contract pads at the top can be used for 4 point measurements. 3 separate transfer lengths are measured; $8.5\,\mathrm{mm}$, $12\,\mathrm{mm}$ and $20.5\,\mathrm{mm}$

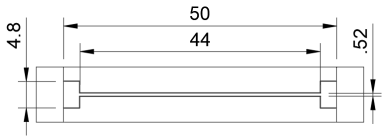


Fig. 2. Piezoresistivity design, dimensions in [mm]

Figure 2 shows the design used for characterising the piezoresistivity. The 2 wider pads at the end are used as contact pads, and the extra substrate at the end is used for clamping the sample.

### B. Fabrication

Printing was done using a Diabase H4 Pro [9], a multimaterial FFF 3D printer, with additional ViscoTec viprohead 3 [10]. This allows for the combined AM process to be performed as a single job task, integrating silver-ink layers into the FFF structures. After printing, the silver ink is cured for 10 minutes at $120\,^{\circ}\mathrm{C}$ in a convection oven [11]. This accelerates the evaporation of the ink solvent, the silver forming the flexible and conductive residue.

TABLE I. Material specific printing parameters

| | Silver-ink | NinjaFlex |
|---|---|---|
| Nozzle temperature [°C] | Room Temperature | 220 |
| Infill density [%] | 100 | 100 |
| Flow [%] | 150 | 120 |
| Print speed [$\mathrm{mm\,s^{-1}}$] | 4 | 25 |
| Printbed temperature °C | 60 | 60 |

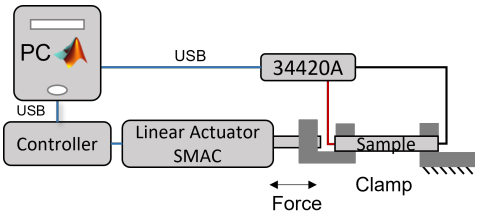


Fig. 3. Experimental measurement setup. Blue line indicates data transfer, red and black the two-point measurement power connections.

Table I shows the final printing parameters, based on experimental optimization. In addition, as a fast retraction at nozzle switch seemed to cause a pressure buildup in the extruder, the retraction speed and amount after extruder switch have been lowered to $5\,\mathrm{mm}$ at $2\,\mathrm{mm\,s^{-1}}$.

## III. Experimental Setup

Figure 3 shows the experimental setup used for the piezo-resistive characterisation. The substrate with ink-trace is clamped with a PolyLactic Acid(PLA) part and mechanically loaded by a mechanical actuator (SMAC LCA25-050, controlled through MATLAB [12]). To readout the resistance a 34420A micro-ohm meter is used (5.5 digits accuracy at $100\,\mathrm{Hz}$ sample rate [13]. To measure the force on the sample the integrated force read-out of the mechanical actuator is used. The MATLAB Parallel Computing Toolbox is used to control the various equipment at a synchronised recording time, with a difference introduced by the (delayed) starting time per parallel job. As means to connect the ink trace to the micrometer, clamps have been designed with the purpose of pressing a copper tape with a width of $6.35\,\mathrm{mm}$ and thickness of $66\mu\mathrm{m}$ on the deposited ink. A coax cable is soldered onto the copper tape to connect to the resistance measurement. This adds contact resistance, however this is small enough to still quantitatively see the piezo resistive effect of the silver.

## IV. Results

### A. Fabrication

Samples with both 1 and 2 layers of silver-ink were fabricated. They are compared in resistance, tensile strength and stability over time when exposed to repeated strains.

Silver ink is extruded as a mixture of silver and solvent. As a result, the actual residue after curing has a smaller volume than when extruded. This shrinking has an influence on the layer thickness and resistivity. To determine the shrinking rate, the samples were fixed to a flat surface with tape and photographed with a micrograph. The result can be seen in 4. A ruler with $0.5\,\mathrm{mm}$ resolution is used as reference. The average linear height shrinking rate of both samples is $70\,\%$. It is also seen that the 2-layer structure has a smoother surface and no clear separation at the layer interface. This observation hints at a low interface resistance, resulting in small or absent anisotropy.

### B. Resistivity

The volumetric resistivity of a material, as determined from a conductive trace, is given by equation 1 where $\rho$ is resistivity [$\Omega\,\mathrm{m}$], $R$ = resistance [$\Omega$], $A$ = area [$\mathrm{m}^2$] and $l$ = sample length [$\mathrm{m}$].

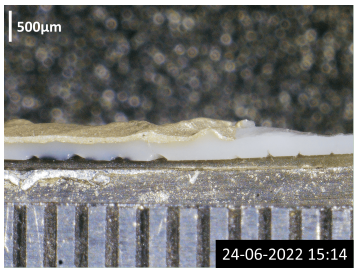


Fig. 4. Silver-ink deposited on TPU square (2 layer)

$$\rho = \frac{R \cdot A}{l} \tag{1}$$

The resistivity of a 2-layer thick silver ink traxel was determined using the transfer length method (TLM), as described in [14]. Figure 5 shows the resistance per transfer length of $0.0036\,\Omega\,\mathrm{mm^{-1}}$ and a contact resistance of $0.010\,\Omega$.

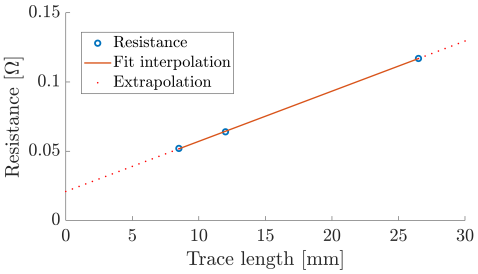


Fig. 5. Resistivity determination by transfer length method

These samples consisted of 1 traxel of ink, 2 layers high, with a width of $0.514\,\mathrm{mm}$ and a layer height of $0.2\,\mathrm{mm}$, see 1. Taking the $70\,\%$ shrinking into account, the cross-sectional area is $0.514\,\mathrm{mm} * 0.4\,\mathrm{mm} * 0.3 = 0.061\,\mathrm{mm}^2$. Using equation 1 gives $\rho$ =$222\,\mathrm{n\Omega\,m}$, which is in accordance with previous research [15] and $5 \cdot 10^5$ lower than CB doped thermoplastic [4].

### C. Piezoresistivity

To characterize the piezoresistivity of the silver ink, a sinusoidal force was applied and the resistance response was measured. An offset of $4.5\,\mathrm{N}$ and an amplitude of $3\,\mathrm{N}$ were used for the excitation with a frequency of 0.2Hz.

To synchronise the signals as measured from the linear actuator and the micro-ohmmeter, a step input is used as to determine a synchronised pulse from all channels. It seems that the standard synchronisation of the parallel computing toolbox is accurate, as figure 6 shows the step input with no time delay compensation applied. This approach assumes that piezoresistive response is instantaneous, at least on the time-scales of our experiments.

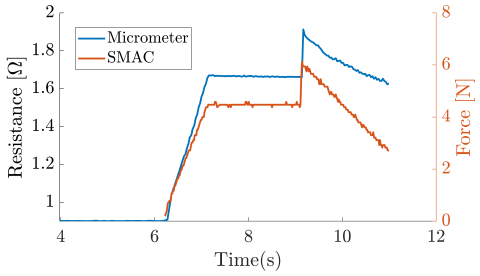


Fig. 6. Step input synchronisation

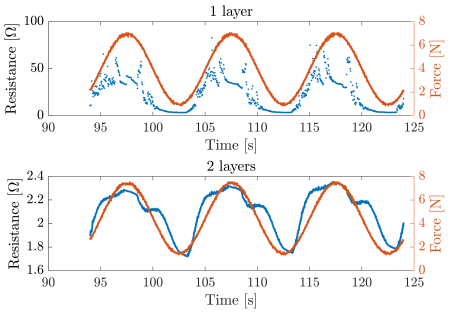


Fig. 7. Resistance response on sinusoidal loading

*1) Sinusoidal loading:* Figure 7 shows the response of both the single and double layer samples. The single layer sample response is monotonous with hysteresis present for low force but has many irregularities for high forces. Sample 2 is the same sample of ink, but tested 5 minutes after the first. The average resistance has increased, and there occurs to be contact loss. The double layer follows the excitation well but has a non-monotonous response on the decreasing part of the excitation.

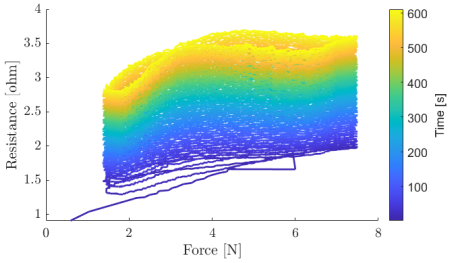


Fig. 8. Resistance vs force on sinusoidal load on a print with 2 layers ink.

Figure 8 shows the resistance vs force response over 600 seconds. It exhibits significant drift, ranging from 1.5 to 3 Ω. This could be caused by the formation of micro-cracks in the silver, slowly increasing the resistance. This was seen in an earlier attempt, where a force higher than 12 N was applied, and crack-formation was observed. The micrograph in figure 9 shows such a crack, where it also was observed that the non-strained resistance increased from 1 Ω to 6 Ω. The irregularities of figure 7 can also stem from this.

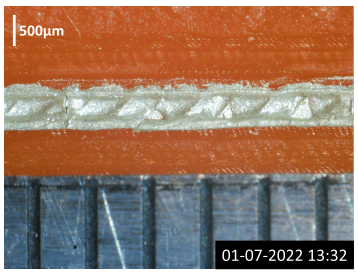


Fig. 9. Crack formed in silver ink

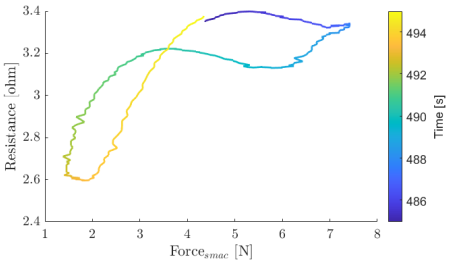


Fig. 10. Single period response

Figure 10 shows a single period response. Here, 2 parts can be identified. The semilinear region below 3.5 N which can be described by the piezoresistivity. For higher force, and thus higher strain, the resistance lowers. The Poisson effect could provide an explanation: the compression in the perpendicular direction could increase the conductivity. Others noted similar behaviour in different materials [16].

## V. Discussion and Conclusion

In this work, the electrical properties of silver-ink and the feasibility for use in sensor fabrication is investigated. First, the silver ink shows a very low electrical resistivity, which is promising for use as contact trace. Secondly, the ink exhibits strong non-linear behaviour at higher strain (>10 %), which limits it's use in piezoelectrical sensing. However, the improved conductivity over carbon doped electrodes can be used beneficially for capacitive sensing. Also, a compressive sensor, to prevent micro-cracks formation in the silver ink layer, might be of better use. Lastly, micrograph pictures show no interfaces between 2 layers of applied silver ink, hinting at a continuous bond in the Z-direction and suggesting a lower anisotropy in electrical properties.

## REFERENCES


[1] M. Schouten, G. Wolterink, A. Dijkshoorn, D. Kosmas, S. Stramigioli, and G. Krijnen, "A Review of Extrusion-Based 3D Printing for the Fabrication of Electro- A nd Biomechanical Sensors," *IEEE Sensors Journal*, vol. 21, no. 11, pp. 12 900–12 912, jun 2021.

[2] P. Jiang, Z. Ji, X. Zhang, Z. Liu, and X. Wang, "Recent advances in direct ink writing of electronic components and functional devices," *Progress in Additive Manufacturing*, vol. 3, no. 1-2, pp. 65–86, jun 2018. [Online]. Available: https://link.springer.com/article/10.1007/s40964-017-0035-x

[3] K. Kim, J. Park, J. hoon Suh, M. Kim, Y. Jeong, and I. Park, "3D printing of multiaxial force sensors using carbon nanotube (CNT)/thermoplastic polyurethane (TPU) filaments," *Sensors and Actuators A: Physical*, vol. 263, pp. 493–500, aug 2017.

[4] A. Dijkshoorn, P. Werkman, M. Welleweerd, G. Wolterink, B. Eijking, J. Delamare, R. Sanders, and G. J. Krijnen, "Embedded sensing: Integrating sensors in 3-D printed structures," *Journal of Sensors and Sensor Systems*, vol. 7, no. 1, pp. 169–181, mar 2018.

[5] Y. Zhang, G. Shi, J. Qin, S. E. Lowe, S. Zhang, H. Zhao, and Y. L. Zhong, "Recent Progress of Direct Ink Writing of Electronic Components for Advanced Wearable Devices," *ACS Applied Electronic Materials*, vol. 1, no. 9, pp. 1718–1734, sep 2019. [Online]. Available: https://pubs.acs.org/doi/full/10.1021/acsaelm.9b00428

[6] P. F. Flowers, C. Reyes, S. Ye, M. J. Kim, and B. J. Wiley, "3D printing electronic components and circuits with conductive thermoplastic filament," *Additive Manufacturing*, vol. 18, pp. 156–163, dec 2017.

[7] L. Del-Mazo-Barbara and M. P. Ginebra, "Rheological characterisation of ceramic inks for 3D direct ink writing: A review," *Journal of the European Ceramic Society*, vol. 41, no. 16, pp. 18–33, dec 2021.

[8] J. K. Wilt, D. Gilmer, S. Kim, B. G. Compton, and T. Saito, "Direct ink writing techniques for in situ gelation and solidification," *MRS Communications*, vol. 11, no. 2, pp. 106–121, feb 2021. [Online]. Available: https://link.springer.com/article/10.1557/s43579-020-00006-8

[9] "Diabase h4 pro." [Online]. Available: https://3dherndon.com/diabase-engineering-5-axis-h-series-hybrid-3d-printer-and-cnc-mill.html

[10] "Vipro head 3." [Online]. Available: https://www.viscotec.de/en/products/3d-print-heads/

[11] Memmert, *Universal oven UF30*, Memmert GmbH + Co. KG, Aeussere Rittersbacher, Strasse 38, D-91126 Schwabach, Germany, 2021. [Online]. Available: www.memmert.com/products/heating-drying-ovens/universal-oven/UF30

[12] M. Schouten, "SMAC_LCA25-5-_MATLAB_driver," 2020. [Online]. Available: https://github.com/martijnschouten/lab-equipment-matlab-drivers/tree/master/SMAC\%20actuator

[13] "34420A User's Guide — Keysight." [Online]. Available: https://www.keysight.com/us/en/assets/9018-01535/user-manuals/9018-01535.pdf

[14] G. Tuttle, *EE 432 : TLM measurements*, Iowa State University, Ames, IA 50011, United States, Mar 2021. [Online]. Available: www.tuttle.merc.iastate.edu/ee432/homepage.htm

[15] F. Tricot, C. Venet, D. Beneventi, D. Curtil, D. Chaussy, T. P. Vuong, J. E. Broquin, and N. Reverdy-Bruas, "Fabrication of 3D conductive circuits: Print quality evaluation of a direct ink writing process," *RSC Advances*, vol. 8, no. 46, pp. 26 036–26 046, 2018. [Online]. Available: https://pubs.rsc.org/en/content/articlehtml/2018/ra/c8ra03380c

[16] J. Yuan, Y. Zhang, G. Li, S. Liu, and R. Zhu, "Printable and Stretchable Conductive Elastomers for Monitoring Dynamic Strain with High Fidelity," *Advanced Functional Materials*, p. 2204878, jun 2022. [Online]. Available: https://onlinelibrary.wiley.com/doi/10.1002/adfm.202204878

# A Appendix 1: 3D printing

## A.1 Design

Design of the samples was done in Autodesk®Fusion 360®. Figure A.1 shows the design for the 4-point measurement. Several design iterations were made and based on printing results the design choices were optimized. During test printing, it was found that 2 layers of silver-ink on top of each other resulted in a more consistent electrical contact. Figure D.2 shows that the resistance of a print with 1 layer is a lot less continuous, and numerous time higher than the double layer. In other measurements, an actual open contact was observed. In addition, corners where the extruder changes direction sometimes break this contact as the adhesion to the previously extruded ink is not as good as a straight line. To isolate the effect of corners, it was chosen to first print 1 layer in a line, without contact pad traces. These contact traces will be printed in the next layer on top, ensuring a good electrical connection, as can be seen in A.2. The line was printed in a trench made of Thermoplastic PolyUrethane(TPU), with a tolerance of 0.1 mm between TPU and silver ink to prevent blending of materials.

## A.2 Slicing

To convert a 3D design into code readable and usable by the 3D printer (Diabase H-series) a so-called *slicing* process is required. This *slices* a 3D design into layers, with each layer having a fixed travel path for the extruder. For this purpose the Cura Slicer is used. The slicing and printing settings can be found in table A.1.

**Table A.1:** Material specific printing parameters

| | Silver-ink | NinjaFlex |
|---|---|---|
| Nozzle temperature [°C] | Room | 220 |
| Infill density [%] | 100 | 100 |
| Flow [%] | 150 | 120 |
| Print speed [$mm\,s^{-1}$] | 4 | 25 |
| Printbed temperature °C | 60 | 60 |

## A.3 Printer

The 3D printer used for manufacturing the samples was a Diabase H4 Pro. It is a multimaterial 3D printer, equipped with Flexion extruders, developed by Diabase. Flexion extruders, in theory, enable increased printing of flexible filaments.

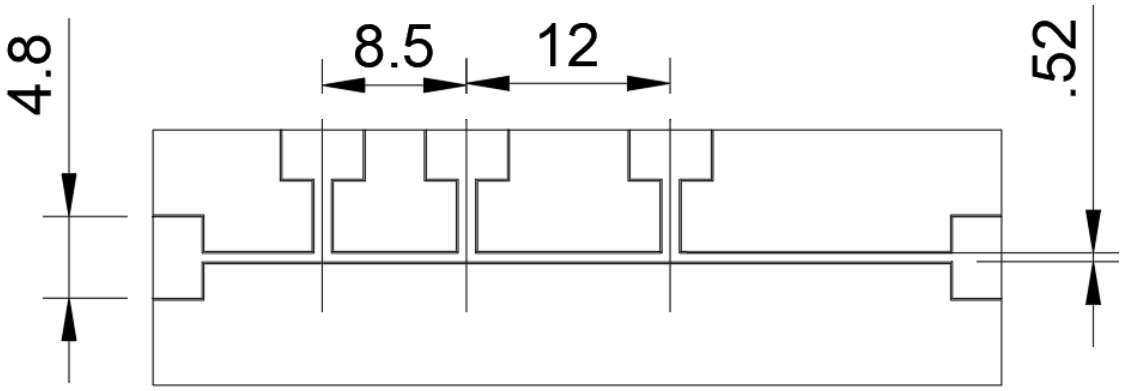


**Figure A.1:** 4 point measurement setup

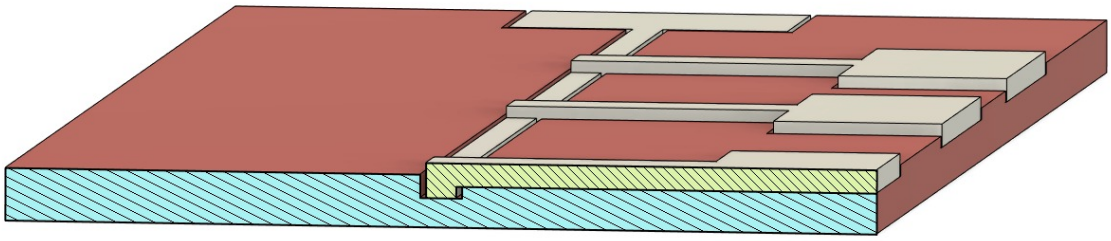

**Figure A.2:** Section view for double layer

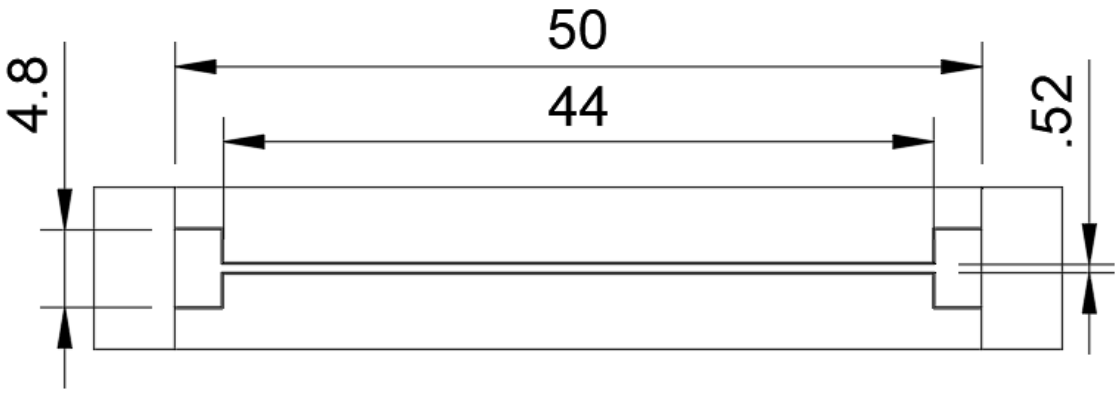


**Figure A.3:** 3D design for resistivity characterization

## A.4 ViscoTec

The Direct-Ink writing of the silver ink, was performed by a ViscoTec Viprohead 3 [1]. It operates under the principle of progressive cavity extrusion for controlled continuous extrusion. Figure A.4 shows the idea of a progressive cavity extruder, or an endless piston. It consists of a thread rotating on . The slicer calculates the path in gcode, and then the printer controls the extruder during printing movement.

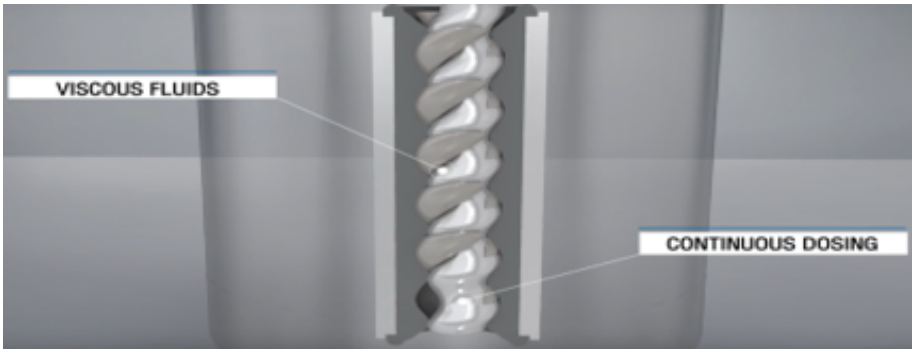


**Figure A.4:** Progressive cavity extrusion principle [1]

## A.5 Sample clamps

Two sets of clamps were designed for use during measurements. The goal of the first set, figure A.5, was to hold the resistivity sample in place, preventing any unwanted strain along the silver ink line. Figure A.6 shows the second set of clamps, that were used for attachment to the base of the measurement setup and to the mechanical actuator used for the loading. These clamps were designed in Autodesk®Fusion360® [2], sliced with PrusaSlicer®and printed on a Prusa MK3S with Polylactic Acid (PLA). PLA is a stiff non-flexible polymer, fit for this application.

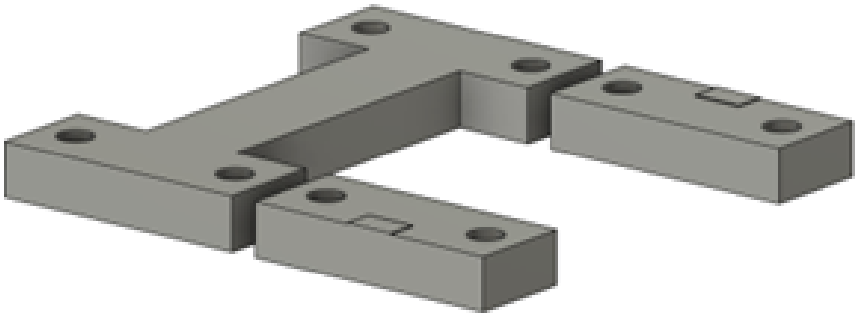

**Figure A.5:** Clamp to fix sample and prevent strain

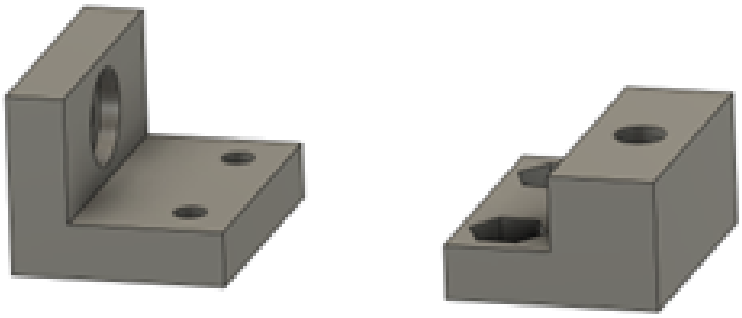

**Figure A.6:** Clamps to attach to mechanical actuator

# B Appendix 2: Measurements

After printing, two measurements were performed. First, the sample resistivity was determined using the transfer length method [3]. The Keithley 34420A 4-point measurement setting was used. To make sure that there was no strain, the first clamp set from section A.5 was used. Copper tape was taped to these clamps, which would be pressed on the contact pads. Wires were soldered to the tape, which acted as the the two current inputs. The voltage measurement wires were attached to the printed sample by means of crocodile clamps as in B.1.

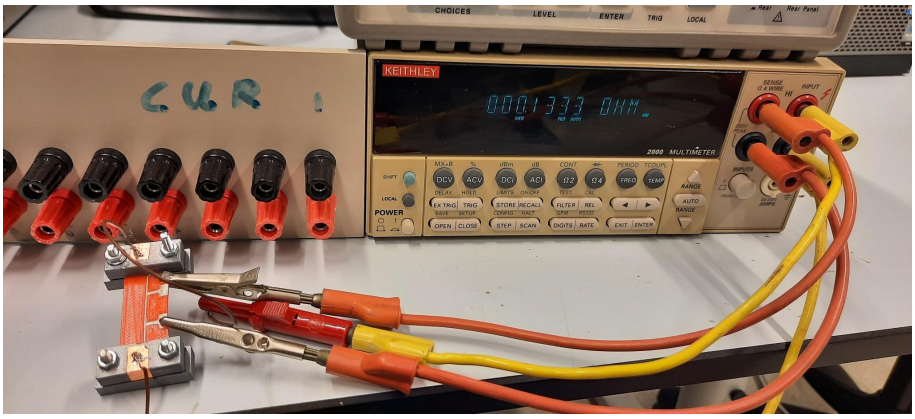


**Figure B.1:** 4 point measurement setup

For the piezoresistive experiment, the setup as seen in figure B.2 was used. To conduct the measurements, the following steps were taken:

- Turn on the SMAC, so it can start the calibration process.
- Set the SMAC to force control and set 0 force, so the sample can be clamped to the setup.
- Turn on the 34420A, and connect all to the measurement workstation.
- Use script *run_parallel.m* in MATLAB C to control the SMAC and micro-ohm meter at simultaneously.

A parallel pool [4] allows for close to perfect synchronization. Supporting functions can be found in *smac_force_control.m, smac_init.m* and *SMAC_read_and_set_force*. Force offset and amplitude, together with frequency of excitation, can be set in *smac_force_control.m*.

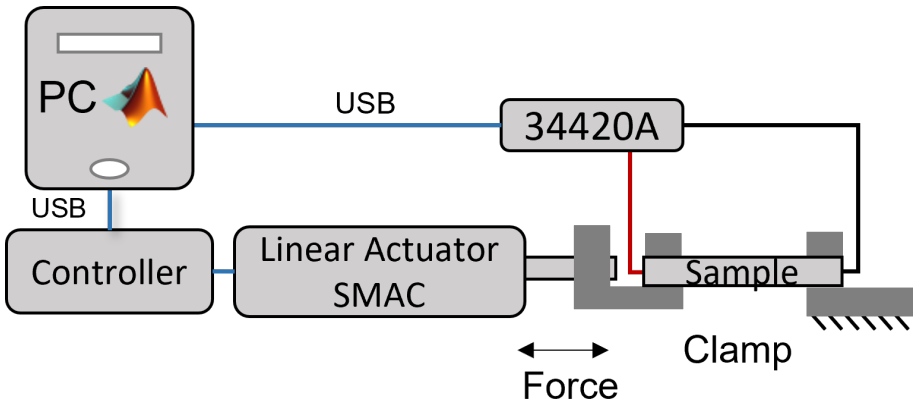


**Figure B.2:** Experimental measurement setup. Blue line indicates data transfer, red and black the two-point measurement power connections.

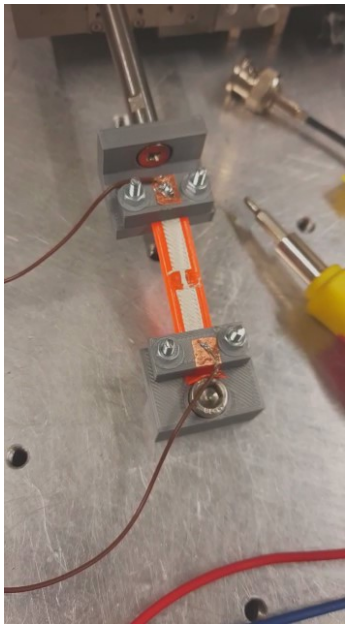

**Figure B.3:** Sample clamped to table(bottom) and mechanical actuator(top)

## B.1 Time synchronisation

As the two measurement devices do not sample at the exact sample rate, synchronisation and downsampling interpolation had to be performed. The achieved sampling frequency of the Micro Ohm meter is 30 Hz, which was lower than the achieved 60 Hz of the SMAC. However, as the excitation frequency was 0.1 Hz, and a lowpass filter with a cutoff at 3 Hz was used, this sampling is more than enough. To eliminate the time delay of the two devices, a ramp input was used in the beginning. This behaviour could be seen in both the force measurement and the resistance measurement, and thus the time delay could be manually removed. To plot the response of resistance against force, measurements had to be on the same time. To do this, linear interpolation from equation B.1 was used to downsample the SMAC measurement and get the interpolated load force at times of the resistance measurements.

$$F = F_1 + \frac{t - t_1}{t_2 - t_1} \cdot (F_2 - F_1) \tag{B.1}$$

With $t_1$, $t_2$, $F_1$ and $F_2$ as the time and force of closest measurements.

# C Appendix 3: Scripts

The following script starts a parallel pool that calls the supporting functions for controlling the measurement equipment. In the parallel for-loop, both functions are called with a tic, the built-in timer in MATLAB. This timer is used to synchronise the measurements, and let them both stop after 600 (= tend) seconds.

```
%% Collect data for SGG capacitive sensor characterization
% Equipment: [1] SMAC actuator (LCA25-050-15SF)
%            [2] Micro-ohm meter (34420A Micro Ohm)
% Author: Dimitris Kosmas

clear
close all

% Preamble ...
    ------------------------------------------------------------------

% Check for open connections
% For [1]
try fclose(actuator); end
% For [2]

% close parallel in case of previous fail
try
    poolobj = gcp('nocreate');
    delete(poolobj);
end

instrreset;

load counter;

% Experiment parameters ...
    ====================================================
tend = 600;

% Measurement loop ...
    ----------------------------------------------------------
parpool(3)
parfor idx = 1 : 3
    tic
    tstart = toc
    utend = toc + tend % add execution time till now
    if idx == 1
        smac_force_control(utend,counter);
    elseif idx == 2
        stream_34420A(utend, counter);
    end
end % Measurement loop end

disp("Measurements finished.")
```

smac_force_control.m starts the connection with the SMAC and waits 5 seconds to give the other streams time to start. After that, it starts with a ramp input of 3 seconds, used to deduce the time-delay between SMAC and other measurements. In the final while loop, the actual excitation sine wave is set to the smac.

```
function smac_force_control(tend,counter) % Check for open connections
     % SMAC related initialization ...
        ========================================
    SMACport = 7;

    actuator = SMAC_init(SMACport); % Call SMAC_init function

    % Smac to force [N] conversion factor (see ram wiki)
    N_perP = 0.0158;
    mm_perP = 0.005;

    % Sinewave
    A = 3/N_perP;
    f = 0.1;
    offset = -4.5/N_perP;

    i1 = 1;
%     force = zeros(1, 60*time);
%     position = zeros(1, 60*time);
%     t_smac = zeros(1, 60*time);
%     Fexcitation = zeros(1, 60*time);

    % Loop the sine wave
    t_start = toc

    while toc < t_start+5
        java.lang.Thread.sleep(0.1*1000)
    end;

    while toc < t_start+5+3
        Fset = offset*min(1,(toc-t_start-5));

        [raw_pos, raw_force] = SMAC_read_and_set_Force(actuator,Fset);

        Fexcitation(i1) = Fset;
        force(i1) = raw_force;
        position(i1) = raw_pos;
        t_smac(i1) = toc;
        i1 = i1 + 1;
    end;

    while toc < tend
        % Put your excitation signal here
        Fset = offset + A * sin(2*pi*f*toc);

        [raw_pos, raw_force] = SMAC_read_and_set_Force(actuator,Fset);

        Fexcitation(i1) = Fset;
        force(i1) = raw_force;
        position(i1) = raw_pos;
        t_smac(i1) = toc;
        i1 = i1 + 1;
    end;

    SMAC_read_and_set_Force(actuator,0);
    force = force.*N_perP;
    position = position.*mm_perP;

    fclose(actuator);

    save(['data/raw/SMAC/','smac_data_',mat2str(counter),'.mat'])
end
```

The following scripts are used for the initialisation and control of the smac, in the specific format needed.

```
function actuator = SMAC_init(port)
%search if there is already a gpib-0-17 object
    actuator = instrfind('Type', 'serial');

    % Create the GPIB object if it does not exist
    % otherwise use the object that was found.
    if isempty(actuator)
        if (port == 0)
            object = instrhwinfo('serial');
            serialPort = object.AvailableSerialPorts{end};
            if serialPort == 1
                warning('error: no serial port found except port 1')
            end
        else
            serialPort = ['COM' num2str(port)];
        end
        actuator = serial(serialPort);
    else
        fclose(actuator);
        actuator = actuator(1);
    end

    %use the \H terminator
    actuator.terminator = 13;
    %set timeout
    actuator.Timeout = 1;
    %set the baud rate
    actuator.baudrate = 115200;

    fopen(actuator);
end
```

```
function [position,force] = SMAC_read_and_set_Force(actuator,force)
if abs(force) ≤ 1000
    if force ≠ 0
        fprintf(actuator,['32 W 0x006071 ' ...
            num2str(int32(force),'%3.0d')])
    else
        fprintf(actuator,['32 W 0x006071 ' num2str(0)])
    end
else
    error('force is out of range')
end
fprintf(actuator, '32 R 0X006064');%read position
fprintf(actuator, '32 R 0X006077');%read force
position = strsplit(fgets(actuator),' ');
position = str2double(position(end));
force = strsplit(fgets(actuator), ' ');
force = str2double(force(end));
```

# D Appendix 4: Additional measurements

Additional measurements were done, but not used in the paper. They will be described here, with their use and comparison to the paper. [5]

Figure D.1 shows a double period response of the design shown in A.1, printed with ETPU instead of silver ink. The load is a sinusoidal load with an offset of 4 N, amplitude of 2 N and frequency of 0.2 Hz It can be seen that the resistance is almost 5000 times higher, but does not show butterfly hysteresis. This hysteresis pattern can be compensated using a model by Dimitris.

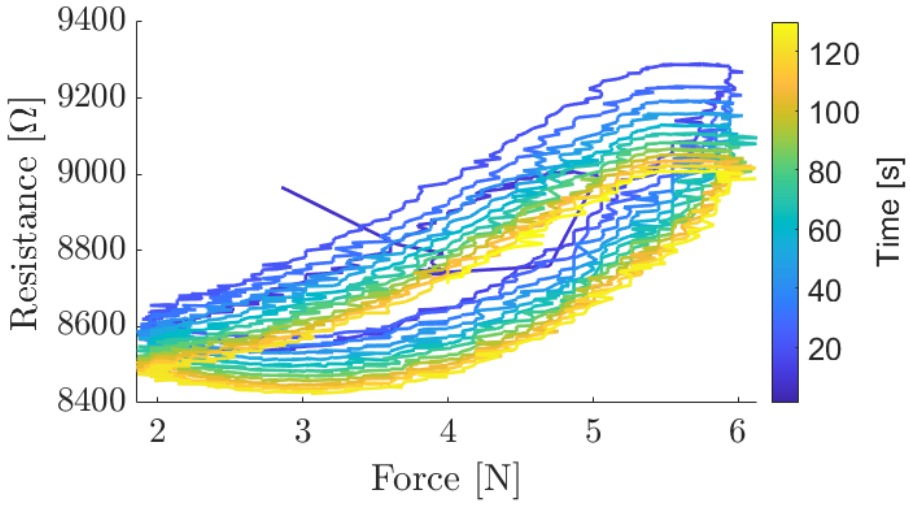


**Figure D.1:** Double period response for ETPU

Figure D.2 shows the resistance-force response of a print with only 1 layer of silver ink. It can be seen that this is very non-linear and has a resistance far higher than the 2-layer silver ink, not explained by the decrease in area. This response is of a sinusoidal load with an offset of 4.5 N, amplitude of 3 N and frequency of 0.1 Hz

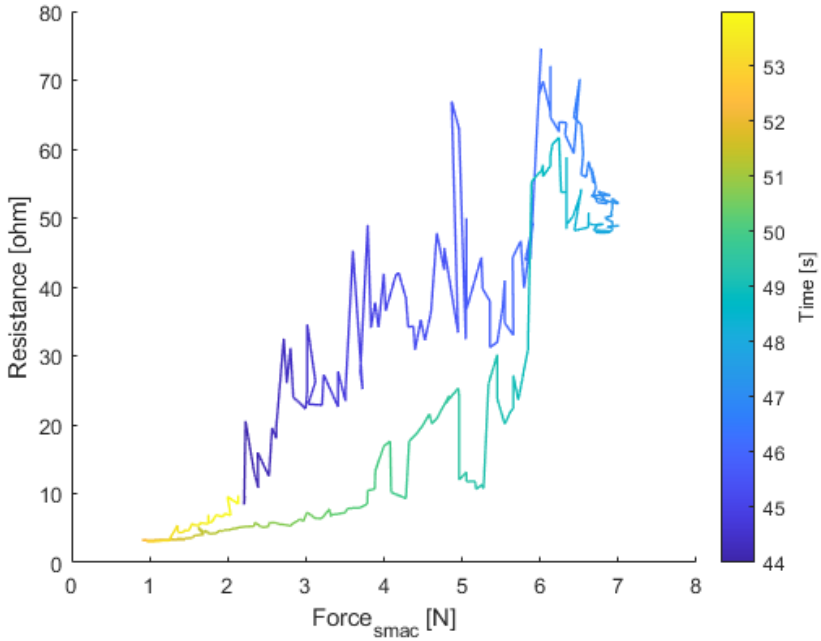


**Figure D.2:** Single period response for silver ink

# Bibliography

[1] "Vipro head 3."

[2] "Cloud powered 3d cad/cam software for product design | fusion 360," 2018.

[3] G. Tuttle, *EE 432 : TLM measurements*. Iowa State University, Ames, IA 50011, United States, Mar 2021.

[4] "Run code on parallel pools, matlab toolbox," 2022.

[5] D. Kosmas, "Model-based hysteresis compensation and control with 3d printed lousy sensors," October 2020.